

Anomalous temperature dependence in the photoemission spectral function of cuprates

C. Kim,* F. Ronning, A. Damascelli, D. L. Feng, and Z.-X. Shen

Department of Physics, Applied Physics and Stanford Synchrotron Radiation Lab., Stanford University, Stanford, California 94305

B. O. Wells, Y. J. Kim, R. J. Birgeneau, and M. A. Kastner

Department of Physics, Massachusetts Institute of Technology, Cambridge, Massachusetts 02139

L. L. Miller

Department of Physics, Iowa State University, Ames, Iowa 50011

H. Eisaki and S. Uchida

Department of Superconductivity, The University of Tokyo, Yayoi 2-11-16, Bunkyo-ku, Tokyo 133, Japan

(Received 12 March 2001; revised manuscript received 6 March 2002; published 23 April 2002)

Temperature-dependent angle-resolved photoemission experiments were performed on overdoped single layer $\text{Bi}_2\text{Sr}_2\text{CuO}_6$ ($T_c \sim 4$ K) and on the parent compounds $\text{Sr}_2\text{CuO}_2\text{Cl}_2$ and $\text{Ca}_2\text{CuO}_2\text{Cl}_2$. Contrary to the more conventional results obtained on $\text{Bi}_2\text{Sr}_2\text{CuO}_6$, the parent compounds show strong temperature dependence over a wide energy range that is two orders of magnitude larger than the temperature scale involved. The doping dependence strongly suggests that the anomalous temperature dependence has its origin in the novel many-body physics in the Mott insulators. We consider the observed temperature dependence using a heuristic model with multiple initial and final states in the photoemission process. The nature of the multiple states and broad photoemission line shape in parent compounds is also given.

DOI: 10.1103/PhysRevB.65.174516

PACS number(s): 71.27.+a, 79.60.Bm

I. INTRODUCTION

It is believed that the doped CuO_2 plane is responsible for high-temperature superconductivity (HTSC). This doped CuO_2 plane shows many peculiar properties that cannot be explained within the simple single-electron picture. The main difficulty is that the relevant electrons experience very large on-site Coulomb repulsion, as they reside in the localized Cu $3d$ orbitals. Even though superconductivity only occurs within a limited doping range of the CuO_2 planes, for a better understanding of the problem it is crucial to study the entire doping range, including the undoped systems (i.e., the so-called parent compounds). In this context, angle-resolved photoemission spectroscopy (ARPES) has proved itself to be an extremely powerful tool. In fact, ARPES studies of $\text{Sr}_2\text{CuO}_2\text{Cl}_2$ and related materials¹⁻⁴ have greatly contributed to the understanding of the electronic structures of the CuO_2 planes.

One of the very interesting observations in spectroscopic studies of transition-metal oxides is the mismatch between the energy scale of the temperature dependence and the temperature involved. For example, optical experiments often show changes up to several electron volts with a temperature change of the order of 100 K.⁵ This mismatch of energy scale by two orders of magnitude cannot be understood by trivial thermal broadening and is likely an indication of many-body processes in the system, and is probably related to anomalous nonconservation of the optical sum rule seen in these materials.⁶ Relatively speaking, much less detailed temperature dependent ARPES experiments were performed on these materials. In most cases, experiments on HTSC materials were performed above and below the superconducting transition temperatures, where the change is observed in a rela-

tively narrow energy range of the order of the gap energy.⁷

Here we report on the anomalous temperature dependence observed in ARPES data from the parent compounds $\text{Sr}_2\text{CuO}_2\text{Cl}_2$ (SCOC) and $\text{Ca}_2\text{CuO}_2\text{Cl}_2$ (CCOC). The comparison of these results with those on single-plane $\text{Bi}_2\text{Sr}_2\text{CuO}_6$ (Bi2201) in the overdoped regime shows dramatic contrast, even though these systems are similar in that they have a single CuO_2 plane per unit cell. Whereas weak temperature dependence is observed on Bi2201, the photoemission (PE) spectral functions of the parent compounds show a very strong and unconventional temperature dependence. It is difficult to explain the strong temperature dependence in the undoped compounds by the simple phonon broadening seen in conventional band materials and the drastic difference in the temperature dependence indicates a rapid change in the many-body effects as one moves away from the boundary of the Mott transition. To account for the energy scale of the temperature dependence as well as the doping dependence, we discuss the transfer of spectral weight considering multiple initial and final states in the PE process. Within this picture, the spectral intensity is transferred from one final state to another upon changing the temperature due to the population shift in the initial states. The implication of this interpretation of the ARPES spectra on the understanding of electronic structures of correlated electron systems is discussed.

II. EXPERIMENT

ARPES data were taken at beamline V of the Stanford Synchrotron Radiation Laboratory. SCOC and CCOC single crystals were grown by the standard solid-state reaction method.⁸ Overdoped Bi2201 with $T_c = 4$ K was grown by

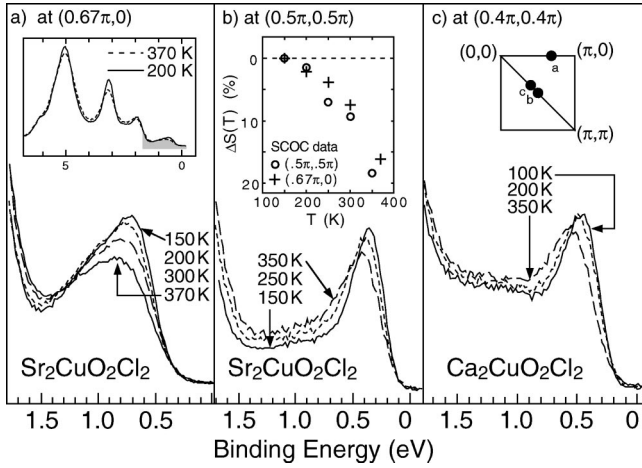


FIG. 1. Temperature-dependent ARPES spectra taken at $(2\pi/3, 0)$ and $(\pi/2, \pi/2)$ on SCOC [panels (a) and (b), respectively] and at $(0.4\pi, 0.4\pi)$ on CCOC [panel (c)]. The three sets of spectra correspond to the little shaded foot structure in the valence-band data shown in the inset of panel (a). The inset in panel (b) shows the percentage change in the integrated low-energy spectral weight $\Delta S(T)$ as defined in the main text. The inset in panel (c) shows the positions in the Brillouin zone where the spectra were taken, with the size of the circles representing the angular resolution.

the traveling-solvent floating-zone method. The crystals were oriented by the Laue method prior to the experiments and then cleaved *in situ* in a pressure better than 5×10^{-11} torr. With 22.4 eV photons, the total energy resolution was typically 70 meV, and the angular resolution was $\pm 1^\circ$. Extreme caution was taken to have fair comparison of the spectra for different temperatures. The data were normalized only by the incident photon intensity. To check the reproducibility and exclude extrinsic effects such as sample aging, experiments were repeated on the same cleaved surface cycling the temperature. Care was taken to ensure that there was no charging problem.

III. EXPERIMENTAL RESULTS

The inset of Fig. 1(a) shows ARPES spectra of SCOC taken at two temperatures. The spectra consist of a wide main valence band with a small foot on the lower binding energy side.¹ The spectra show strong temperature dependence over the entire valence band. While we believe the temperature dependence seen on the main valence band is due to the same effect that will be discussed later, it is more complicated in the case of the main valence band because it has multiple bands. We thus concentrate on the foot structure which has a single band character according to the band structure calculations.⁹ Figures 1(a) and 1(b) show the low-energy part of ARPES spectra from SCOC for several temperatures and two different \mathbf{k} -space points in the first Brillouin zone (BZ), as indicated in the inset in Fig. 1(c). The detected peaks are often referred to as the quasiparticle peaks and are the states with $d_{x^2-y^2}$ symmetry from the CuO_2 plane. What catches one's eye is the large temperature dependence over a large energy scale, more than 1 eV which is two orders of magnitude larger than the temperature in-

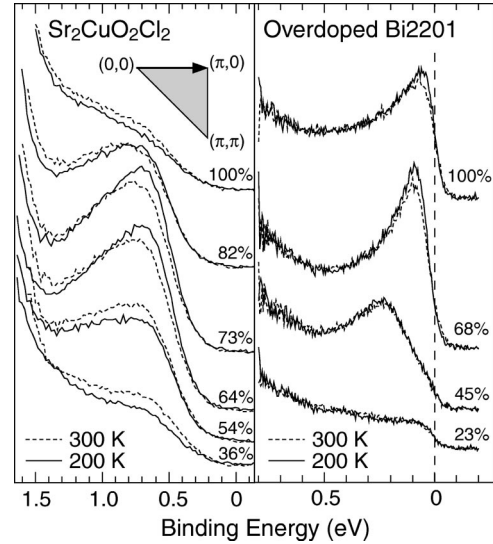


FIG. 2. Comparison of temperature-dependent ARPES spectra along the $(0,0)$ to $(\pi,0)$ cut on SCOC and overdoped Bi2201. The number on each spectra shows the distance from $(0,0)$ to the $(\pi,0)$ point in percentage. The spectra have been normalized only by the incident photon intensity. Note that the energy scales for the two panels are different.

involved. For both points in the BZ, upon lowering the temperature, the peak becomes stronger and sharper, and shifts to lower energies (note that the observed peak shift is not due to charging of the sample as it would shift the peaks in the opposite direction). Even the higher-binding-energy side which has often been regarded as background shows a strong temperature dependence. Figure 1(c) presents a set of spectra taken at $(0.4\pi, 0.4\pi)$ on the similar compound CCOC, for several temperatures. As shown by a direct comparison between Figs. 1(b) and 1(c), the spectra of SCOC and CCOC display qualitatively the same behavior. To quantify the temperature dependence, the normalized low energy spectral weights for SCOC defined as $\Delta S(T) = \int [I(T, E)/I(150, E)] - 1 dE$ are plotted in the inset of panel (b). Here $I(T, E)$ is the photoemission intensity at temperature T and energy E . The integration windows for $(2\pi/3, 0)$ and $(\pi/2, \pi/2)$ are 1.2 eV and 0.45 eV, respectively. The exact values of the energy windows do not affect the overall behavior of the temperature dependence.

To further investigate this issue, we performed temperature dependence measurements on overdoped Bi2201 ($T_c = 4$ K) and compared the data to those on SCOC. Both of these materials have very similar CuO_2 planes and their electronic properties are extremely two dimensional. The essential difference between the two is the doping, with the overdoped Bi2201 having effectively smaller electron-electron correlations. The idea is to test if the anomalous temperature dependence seen in Fig. 1 is related to many-body effects that change with doping. In addition, doping dependence studies in cuprates quite often provide insightful information. The results are shown in Fig. 2 for several selected \mathbf{k} -space points along the $(0,0)$ to $(\pi,0)$ cut for 200 K and 300 K. The contrast is striking and represents the most convincing evidence that the temperature dependence observed on SCOC

and CCOC is due to many-body effects in the Mott insulators that go away with doping. While a very strong temperature dependence is seen at different k points on SCOC, Bi2201 shows a weak temperature dependence similar to what one would expect from thermal broadening in a simple metal, with the most evident effect being the weak decrease of peak intensity upon increasing temperature.

IV. INTERPRETATION BY SPECTRAL WEIGHT TRANSFER

A. Failure of the conventional interpretations

There are conventional ways to explain the temperature dependences seen in photoemission spectra. The first is thermal smearing due to the Fermi-Dirac statistics. The effect results in broadening of a Fermi step by $\approx 4kT$. This is purely electronic in origin and applies only to the states near the Fermi energy as the effect is negligible once the states are away from the Fermi energy. Hence, the temperature dependence seen in Fig. 1 cannot be the thermal smearing effect. A more common explanation for the temperature-dependent photoemission spectra is the simple phonon broadening. Here we emphasize that, by saying “simple phonon broadening,” we refer to the case of band electrons interacting with phonons as seen in *conventional band materials*. Indeed, such an effect is expected in PE spectra similar to what is found in neutron and x-ray scattering¹⁰ where the decreased intensities of diffraction peaks upon increasing temperature are described by the Debye-Waller factor e^{-2W} (where $W \propto T$). In addition, the simple phonon effect is also responsible for a (weak) temperature-dependent shift and broadening of the PE peaks.¹⁰ However, there are reasons why the behavior shown in Fig. 1 is difficult to reconcile with pure phonon effects that are observed on conventional systems (systems with noncorrelated electrons). First, the energy scale is larger than the phonon energy scale. For the simple phonon effect, one expects a broadening of the peak $\Delta E_{width} = 2\pi\lambda k_B \Delta T$ ($k_B \Delta T \sim 25$ meV for $\Delta T = 300$ K) where λ is the electron-phonon coupling parameter and ΔT is the temperature change.¹¹ The electron-phonon coupling parameter λ is usually less than 1 [$\lambda = 1.15$ for Be(0001) surface states which have very strong electron-phonon coupling] and is expected to be smaller for band insulators.¹¹ Therefore, such a strong temperature dependence over a large energy scale shown in Fig. 1 is unlikely to be induced by the simple phonon broadening. Another fact that is not consistent with the simple phonon effect for the observed temperature dependence is the peak position shift ΔE_{peak} . In Fig. 1 we can observe $\Delta E > 100$ meV for $\Delta T \approx 200$ K, whereas the energy shift due to a simple phonon effect is at most 50 meV.^{10–12} Second, the intensity change in Fig. 1 is much more than what one would expect from a simple phonon effect in a single-band material.^{10–12} An apparent exception is a comparable intensity change observed on Au(111) (Ref. 13); it is, however, due to the reduction of the photoelectron diffraction signal by phonons and thus observed only for a special k point (normal emission), unlike the present case. In addition, some of the SCOC spectra in the left panel of Fig. 2 (the top and the two bottom sets) gain

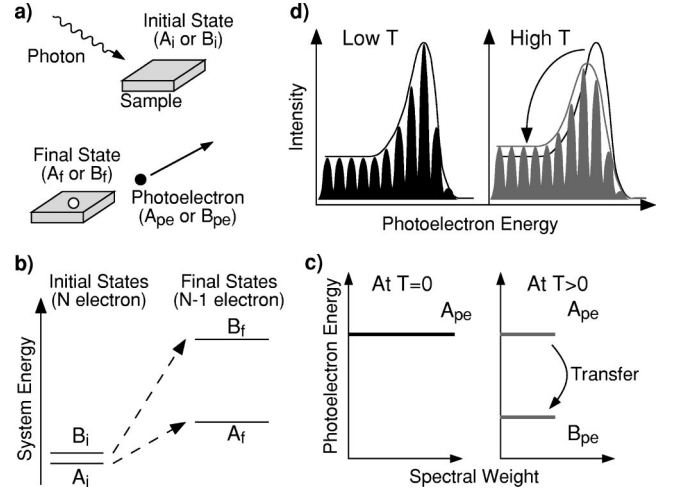


FIG. 3. Panel (a): Sketch of the PE process. Panel (b): Model system to discuss the spectral weight transfer. The system has initial states A_i and B_i , and final state A_f and B_f . Only transitions from A_i to A_f , and from B_i to B_f are allowed. The resulting PE spectra at different temperatures are depicted in panel (c). As shown in panel (d), the shift of peak position observed in the experiment (Fig. 1) can now be understood as transfer of spectral weight due to the existence of multiple initial and final states.

spectral weight as the temperature is increased. This is unexpected on the basis of simple phonon broadening because thermally excited phonons only reduce the spectral weight of the PE feature.¹⁰

B. Overall view of spectral weight transfer

The contrasting behaviors in the data from SCOC and Bi2201 indicate that the anomalous temperature dependence seen in the SCOC data is due to a many-body effect. Within this framework, it is possible to construct a heuristic model to account for the large energy scale temperature dependence on insulating systems by considering the spectral weight transfer between *multiple final states* (whose nature will be discussed below) in the PE process. To understand the spectral weight transfer, one cannot use a simple view of PE as a direct mapping of band structure. Instead, one must use the general view of PE as an excitation process of a system from an initial state to a final state and a photoelectron as depicted in Fig. 3(a). Measurements of the energy and momentum of the photoelectron give the energy and momentum of the $N - 1$ electron final state through the conservation laws

$$k_i = k_{pe} + k_f \quad (\text{momentum conservation}), \quad (1)$$

$$h\nu + E_i = E_{pe} + E_f \quad (\text{energy conservation}), \quad (2)$$

where $h\nu$ is the energy of the photon, k_{pe} , k_i , k_f , E_{pe} , E_i , and E_f are momenta and energies of the photoelectron and initial and final states, respectively (here “state” refers to a state of the whole system, not to a one-electron state).

Let us consider an idealized system as the one depicted in Fig. 3(b). Before the PE process, we have two initial states A_i and B_i , very close in energy. After the PE process, we also have two final states (A_f and B_f , with one fewer elec-

tron compared to A_i and B_i) which are, contrary to the initial states, far apart in energy. Now let us assume the transition from A_i (B_i) to A_f (B_f) is allowed but is disallowed to B_f (A_f), due to the *different symmetry* of A_i and B_i in regard to the *dipole selection rule*. At 0 K, the probability of the system being in state A_i is 1 and in B_i is 0, according to Boltzman statistics [Fig. 3(c)]. As a result, only the photoelectrons (A_{pe}) corresponding to the final state A_f are emitted. Note that the photoelectron A_{pe} has energy higher than B_{pe} because of energy conservation. When the temperature of the system increases, the probability of finding the system in state B_i increases too, and hence we begin to see transitions to state B_f . That is, spectral weight is *transferred* from A_f to B_f . Note that the state B_f can be energetically quite separated from the state A_f , and this energy scale is not related to the temperature scale $k_B T$ (the latter only controls the initial-state distribution) and in principle can be orders of magnitude larger. What is described here is an idealized case. In reality, A_i (B_i) would have a finite transition amplitude to B_f (A_f) too. But if there is any imbalance in transition probabilities, a sizable spectral weight transfer will be observed. Indeed, numerical studies based on many-body theory show a temperature dependence in ARPES spectral functions with energy scale much larger than the temperature scale.^{14,15} This effect is also relevant for other spectroscopic methods, such as optical measurements, to explain the observed temperature dependencies.^{34–36,5}

C. Multiple final states

A necessary condition for this mechanism to work over a large energy scale is the existence of multiple final states (A_f and B_f in the example) spread over a wide energy range for a given momentum \mathbf{k} . This is unexpected with a simple view of ARPES as direct transition between the rigid electronic bands, which works only in the noninteracting electron picture in a strict sense. With electron correlation, a possible distribution of the final states over a wide energy range can be described in the following way. For simplicity of the discussion, we start with a simple noninteracting electron system in the ground state. As stated earlier, in a rigorous sense, the PE process should be understood as a transition between initial and final states of the *system*. Figure 4(a) depicts an initial state (ground state for simplicity) of a noninteracting electron system. In panel (b), a possible final state of the $(N-1)$ -electron system is shown. The energy and momentum of the photoelectron can be obtained according to Eqs. (1) and (2). The resulting PE states (states in phase space that the photoelectron can occupy) are plotted in the same panel. Note that, in the final state of the $(N-1)$ -electron system, the only difference is in one of the initially occupied single-electron states (type I). The PE states associated with type-I final states are the usually perceived PE states and they reproduce the initial one-electron band. For this reason, ARPES is often referred to as a mapping of the band structure. However, there is no *a priori* reason why only the type-I final states shown in panel (b) should be considered. For example, if we consider a final state of the $N-1$ system with an electron-hole pair in addition to the photohole as

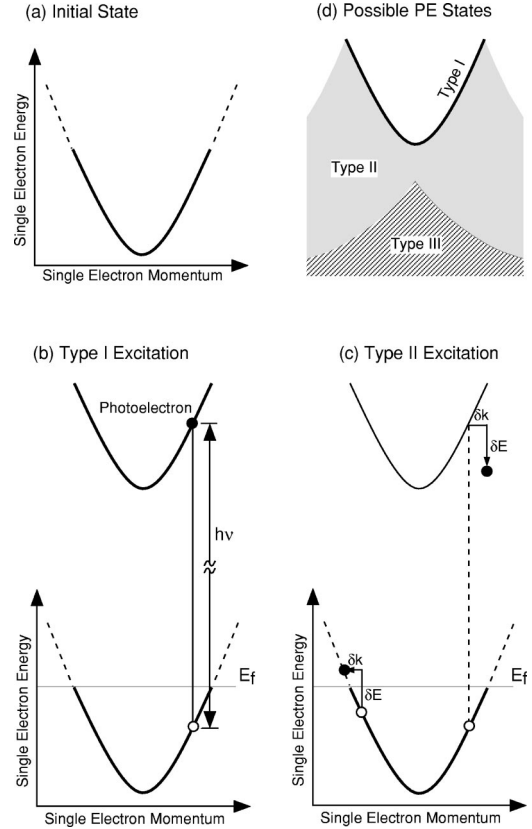


FIG. 4. (a) The initial (ground) state of a noninteracting electron system. (b) A final state with only one electron removed (type I) and the resulting PE state. (c) Another possible final state with an electron-hole pair in addition to the photohole. The resulting photoelectron is not on the “band.” (d) Regions of phase space where possible PE states exist. Type III is a superset of type II, but labeled as shown in the figure for clarity.

shown in panel (c) (type II), the resulting PE state is not on the “band” [the PE states in panel (b)] but away from it to satisfy the energy and momentum conservation laws. Likewise, we can consider two electron-hole pairs (type III) and proceed to construct all the possible final and corresponding PE states. The possible PE states constructed this way are shown in panel (d). The thick line represents the PE states with the type-I final states depicted in panel (b). The gray area represents the PE states with the type-II final states shown in panel (c) while the hatched area represents type-III states [note here that type II is a subset of type III, but it is shown as in panel (d) for clarity].

As is shown above, there can be multiple PE states over a wide energy range for a given momentum \mathbf{k} . This is due to the fact that the photoelectron reflects the properties of the *many-body system*. It is, however, important to note that only the type-I states have *spectral weight* (transition probability) and thus are observable in the case of noninteracting electron systems. That is, only a single state is *observed* for a given \mathbf{k} for a noninteracting electron system. In the case of interacting electron systems, the system wave functions can no longer be expressed as a single Slater determinant and other states such as type II will have spectral weight.¹⁶ In this case, a broad distribution of PE states for a given \mathbf{k} will appear

and the breadth of the observed spectral feature consisting of such multiple states is related to the strength of the correlation. In a single-particle description of the excited states of the many-body system such as Fermi liquid theory, this breadth is interpreted as the lifetime of the quasiparticle.^{17–20} These multiple states appear due to the electron correlation or configuration interaction. This effect also causes the satellite structures, shakeoffs, and shakeups observed in the photoemission spectroscopy.^{10,21–23}

Calculations based on many-body theory (such as Hubbard or t - J models) with realistic parameters for cuprates show multiple final states spread over the several eV energy range, supporting the discussion above.²⁴ Electron correlation plays an important role in this new interpretation by allowing multiple final states over wide energy range. Such multiple states are observed in the data shown in Fig. 1(a): the peak is very asymmetric and appears to have a second structure at ~ 1.2 eV binding energy. Spectra taken at certain k -space points show the second feature and additional higher energy states more clearly than others.²⁴ The two features in the data in Fig. 1 constitute just part of the final-state spectral weight, with the rest of it being buried under the main valence band at higher energies according to numerical results.²⁴ The shift of the peak position seen in Fig. 1 may further imply that even the peak—for example, shown in Fig. 1(c)—may consist of multiple final states as some theoretical work suggests.²⁵ In this case, the breadth of the peak is due to the existence of multiple final states rather than an extremely short photohole lifetime as mentioned above.²⁶ The peak shift can then be understood as the consequence of the transfer of spectral weight as illustrated in Fig. 3(d). As temperature increases, the lower-energy states are suppressed and the spectral weight is transferred to higher-energy states. The peak appears to move to the higher-energy side even though the positions of the final states do not move. Within this interpretation, the peak position is not the position of a state, but simply the centroid of a multiple-state structure.

In regards to the broadness of the lowest-energy peak discussed above, numerical results based on the t - J model show the lowest-energy peak always standing out independent of the cluster size similar to a sharp quasiparticle peaks.^{24,27} This is quite different from what is observed experimentally where the width of the lowest-energy peak is at least 300 meV as shown in Fig. 1. One of the explanations may be that t - J is a very simplified Hamiltonian and cannot explain the experimental results. Indeed, calculated spectra of the one-dimensional (1D) system based on a more realistic Cu-O ring show more states, making the features broader compared to simple t - J results.²⁸ Another possibility is from the role of phonons. Theoretically it was found that incorporating phonons into t - J calculations greatly increases the width of calculated Raman spectra, with the magnons providing the energy scale and phonons providing coupling between different states.²⁹ A similar mechanism may be responsible for the broad line shape in photoemission spectra with the phonons giving the coupling between the multiple states described above. It is unclear which one is more responsible and we leave this as an open question for future studies. In either

case, the interpretation of the temperature dependence by spectral weight transfer is largely unaffected.

D. What are the initial states?

Possible candidates for the initial states depicted in Fig. 3 may result from instabilities leading to charge and spin ordering in many transition-metal oxides. Indeed, ARPES results on Zn-doped $\text{Bi}_2\text{Sr}_2\text{CaCu}_2\text{O}_8$ (Zn is believed to favor magnetic ordering in this material) show an enhanced temperature dependence compared to the Zn-free case.³⁰ Optical measurements on unreduced $\text{Nd}_{2-x}\text{Ce}_x\text{CuO}_4$ also show that spin and charge instabilities can cause a strong temperature dependence.⁵ Since there are no such instabilities in SCOC and CCOC, the natural question is, what are the initial states that are energetically close and give different transition probabilities (due to different symmetries) for the final states? One obvious candidate is the phonons. As discussed before, numerical work based on many-body theory shows that inclusion of phonons greatly increases the ARPES linewidth, which in turn means the phonon states are bridged to different final states (note again that the phonon energy scale is relevant only to the initial energy scale with the large final-state energy scale being provided by the electron-electron correlation and this picture thus differs from simple phonon broadening). Even though temperature dependence studies based on the t - J model without phonons show a very large energy scale, the degree of the temperature dependence is much smaller than the experimental observation shown in Fig. 1.¹⁴ It was found that inclusion of phonons in this model enhances the temperature dependence in addition to giving the broad width which was difficult to produce.³¹ At low temperature, the system is more likely to be in the ground state. At a higher temperature, the probability of the system to be in a thermally excited phonon state increases, resulting in a redistribution of the spectral weight in different final states.

Another possibility comes from the the low-energy spin-flipped states in SCOC and CCOC. These spin excitation states may be the initial states with different symmetries. Turning our attention to the data shown in Fig. 2, we know that the difference between SCOC and Bi2201 is essentially the doping level. Upon increasing doping the antiferromagnetic (AF) correlations decrease. On the very overdoped side the CuO_2 plane becomes an almost paramagnetic system; that is, magnetism is very weak.³² These results from SCOC and CCOC along with the Bi2201 case therefore may suggest that magnetism is related to the strong temperature dependence seen in ARPES spectra of SCOC and CCOC. As discussed above, these states may be bridged to different final states by the dipole selection rule, hence strongly affecting the ARPES line shape as the probability of thermally excited spin states increasing at higher temperature. This means that the *magnetism* in these systems may be responsible for the anomalous temperature dependence.

The idea that magnetism greatly contributes to the strong temperature dependence is supported by other experimental results. ARPES spectra on $\text{La}_{2-x}\text{Sr}_x\text{Mn}_3\text{O}_7$ (Ref. 33), as well as optical measurements on SCOC,³⁴ $\text{YBa}_2\text{Cu}_3\text{O}_6$,³⁵ and

FeSi,³⁶ suggest that the magnetism contributes to strong temperature dependence over a large energy scale. In particular, a detailed analysis of the bimagnon-plus-phonon spectrum of $\text{YBa}_2\text{Cu}_3\text{O}_6$ (Ref. 35) and SCOC (Ref. 37) not only suggests the magnetism as an essential part of the observed optical absorption, but also indicates that the continuum of excitations extending to very high energy (~ 1 eV) is due to spin fluctuations (the higher the temperature, the more severe they are), which are responsible for strong local deviations from the Néel state in 2D undoped cuprates. One particular prediction of this interpretation is that the strong temperature dependence should disappear when the system becomes paramagnetic at high temperature. Supporting evidence for this picture may be the temperature-dependent optical measurements on unreduced $\text{Nd}_{2-x}\text{Ce}_x\text{CuO}_4$. The measurements show that the temperature dependence disappears above 340 K when the system becomes uniform.⁵ For SCOC and CCOC ($T_N=256$ K), however, this temperature is too high for ARPES measurements. The data in the inset of Fig. 1(b) appear to show a slope change around T_N similar to the optical data on SCOC,³⁴ but the energy window is not large enough to make a concrete conclusion. Therefore, experiments on an AF system with a small J (small enough to access the paramagnetic state) as well as on insulating 2D nonmagnetic samples should be important to verify our attribution of the strong temperature dependence to magnetism.

In the above, we proposed phonons and low-energy magnetic excitations as the possibilities for the initial states in SCOC and CCOC. Even though which one contributes more is an interesting question, it is worth noting that separating the two cases may not be possible: there is no crystalline system that does not have phonons and correlated systems considered here mostly have magnetism. Therefore, experimentally finding out which is more responsible is a very difficult task and may only be possible theoretically. More importantly, it may also be that we need both of them to have the observed anomalous temperature dependence; that is, magnetism and phonons play on top of each other to produce such a strong temperature dependence as was suggested in the bimagnon-plus-phonon analysis.^{35,37} In this regard, it is interesting to note that a strong doping dependence of the electron-phonon coupling in cuprates has been argued in a recent report.³⁸

V. CONCLUDING REMARKS

The broad ARPES line shape observed on HTSC's, especially in the underdoped case, has often been attributed to an

extremely short photohole lifetime (hence extremely short mean free path).^{19,20} However, there is a strong discrepancy between the lifetime directly measured³⁹ in pump-probe experiments ($\hbar/\tau < 10$ meV) and the one inferred from the linewidth of ARPES spectra (~ 300 meV). In addition, recent measurements of the thermal Hall conductivity also suggest a very long mean free path, about 200 times longer than what is inferred from the sharpest ARPES peak.⁴⁰ As discussed above, a “peak” consists of multiple states and its width does not reflect the photohole lifetime (physical time) but the strength of correlations which give rise to the multiple states. This naturally explains the general trend of broader spectral features towards insulating states.⁴¹ More importantly, the observed temperature-dependent redistribution of spectral weight suggests that the multiple states within the peak may have different properties and hence the single-particle description of the excited states fails, the possibility of which was raised soon after HTSC was discovered.⁴²

In summary, we performed temperature-dependent ARPES measurements on single-plane cuprates. Whereas the spectra on overdoped Bi2201 show a rather weak temperature dependence, in the insulating parent compounds SCOC and CCOC we observed a very strong temperature dependence (both in energy and intensity), which is not expected in a noninteracting electron picture. This indicates that many-body effects originating from the strong electron correlations characterizing the CuO_2 plane have to be taken into account. Phonons and magnetic excitations are discussed as possible candidates for the low-energy initial states. We show that the anomalous temperature dependence can be accounted for by considering the transfer of spectral weight between multiple initial and final states in the photoemission process. In this context, only the initial-state configuration is inherent to the experimental temperature scale. What is discussed in this paper has important implications for the understanding of not only the ARPES line shapes but also data from other spectroscopic methods in correlated electron systems.

ACKNOWLEDGMENTS

We gratefully acknowledge helpful discussions with T. Tohyama, S. Maekawa, Z.-Y. Weng, N.P. Armitage, E. Dagotto, J. van den Brink, and G. A. Sawatzky. SSRL is operated by the DOE office of Basic Energy Research, Division of Chemical Sciences. The office's division of Material Science provided support for this research.

*Present address: Institute of Physics and Applied Physics, Yonsei University, Seoul, Korea. Electronic address: cykim@phya.yonsei.ac.kr

¹B.O. Wells, Z.-X. Shen, A.Y. Matsuura, D.M. King, M.A. Kastner, M. Greven, and R.J. Birgeneau, *Phys. Rev. Lett.* **74**, 964 (1995).

²C. Kim, A.Y. Matsuura, Z.-X. Shen, N. Motoyama, H. Eisaki, S. Uchida, T. Tohyama, and S. Maekawa, *Phys. Rev. Lett.* **80**, 4245 (1998).

³S. LaRosa, I. Vobornik, F. Zwick, H. Berger, M. Grioni, G. Margaritondo, R.J. Kelley, M. Onellion, and A. Chubukov, *Phys. Rev. B* **56**, R525 (1997).

⁴F. Ronning, C. Kim, D.L. Feng, D.S. Marshall, A.G. Loeser, L.L. Miller, J.N. Eckstein, I. Bozovic, and Z.-X. Shen, *Science* **282**, 2067 (1998).

⁵Y. Onose, Y. Taguchi, T. Ishikawa, S. Shinomori, K. Ishizaka, and Y. Tokura, *Phys. Rev. Lett.* **82**, 5120 (1999).

⁶D.N. Basov, S.I. Woods, A.S. Katz, E.J. Singley, R.C. Dynes, M.

- Xu, D.G. Hinks, C.C. Homes, and M. Strongin, *Science* **283**, 49 (1999).
- ⁷A. Damascelli, D.H. Lu, and Z.-X. Shen, *J. Electron Spectrosc. Relat. Phenom.* **117-118**, 165 (2001).
- ⁸L.L. Miller, X.L. Wang, S.X. Wang, C. Stassis, D.C. Johnston, J. Faber, and C.K. Loong, *Phys. Rev. B* **41**, 1921 (1990).
- ⁹D.L. Novikov, A.J. Freeman, and J.D. Jorgensen, *Phys. Rev. B* **51**, 6675 (1995).
- ¹⁰S. Hüfner, *Photoelectron Spectroscopy: Principles and Application* (Springer-Verlag, New York, 1995).
- ¹¹T. Balasubramanian, E. Jensen, X.L. Wu, and S.L. Hulbert, *Phys. Rev. B* **57**, R6866 (1998).
- ¹²J. Fraxedas, J. Trodahl, S. Gopalan, L. Ley, and M. Cardona, *Phys. Rev. B* **41**, 10 068 (1990).
- ¹³R. Matzdorf, R. Paniago, G. Meister, A. Goldmann, C. Zubragel, J. Braun, and G. Borstel, *Surf. Sci.* **352-354**, 670 (1996).
- ¹⁴Y. Shibata, T. Tohyama, and S. Maekawa, *Phys. Rev. B* **59**, 1840 (1999).
- ¹⁵R. Preuss, W. Hanke, C. Grober, and H.G. Evertz, *Phys. Rev. Lett.* **79**, 1122 (1997).
- ¹⁶T. Tohyama *et al.* (unpublished). Exact diagonalization results of 1D Hubbard model show, in addition to the change in the spectral weight of the states, the shape of the region of PE states changes as the correlation increases. Also the distinction between the different types of excitations becomes less well defined with the correlation.
- ¹⁷In the context of the discussion given here, even the quasiparticle peak in Fermi liquid theory should be thought of as collection of multiple states, with the width of the peak as a fictitious lifetime. In that case, the validity of Fermi liquid picture depends on whether the states within the peak behave similarly so that the peak (collection of multiple states) can be approximated by a peak with a certain fictitious lifetime broadening. See C. Kim, *J. Electron Spectrosc. Relat. Phenom.* **117-118**, 503 (2001).
- ¹⁸W.B. Jackson and J.W. Allen, *Phys. Rev. B* **37**, 4618 (1988).
- ¹⁹T. Valla, A.V. Fedorov, P.D. Johnson, B.O. Wells, S.L. Hulbert, Q. Li, G.D. Gu, and N. Koshizuka, *Science* **285**, 2110 (1999).
- ²⁰A. Kaminski, J. Mesot, H. Fretwell, J.C. Campuzano, M.R. Norman, M. Randeria, H. Ding, T. Sato, T. Takahashi, T. Mochiku, K. Kadowaki, and H. Hoehst, *Phys. Rev. Lett.* **84**, 1788 (2000).
- ²¹R.L. Martin and D.A. Shirley, *J. Chem. Phys.* **64**, 3685 (1976).
- ²²H. Tjeng, Ph.D. thesis, University of Groningen, 1990.
- ²³L. Ley and M. Cardona, *Photoemission in Solids* (Springer-Verlag, Berlin, 1979), Vol. II.
- ²⁴E. Dagotto, *Rev. Mod. Phys.* **66**, 763 (1994).
- ²⁵D.N. Sheng, Y.C. Chen, and Z.Y. Weng, *Phys. Rev. Lett.* **77**, 5102 (1996).
- ²⁶Here the multiple states can have contribution from phonons but suggesting the energy scale of the phonon scattering process is relatively small. The possible role of the phonons is discussed below.
- ²⁷G.B. Martins, C. Gazza, and E. Dagotto, *Phys. Rev. B* **59**, 13 596 (1999).
- ²⁸T. Tohyama *et al.* (unpublished).
- ²⁹F. Nori, R. Merlin, S. Haas, A.W. Sandvik, and E. Dagotto, *Phys. Rev. Lett.* **75**, 553 (1995).
- ³⁰P.J. White, Z.-X. Shen, D.L. Feng, C. Kim, M.Z. Hasan, J.M. Harris, A.G. Loeser, H. Ikeda, R. Yoshizaki, G.D. Gu, and N. Koshizuka, cond-mat/9901349 (unpublished).
- ³¹S. Yunoki (private communication).
- ³²R.J. Birgeneau, D.R. Gabbe, H.P. Jensen, M.A. Kastner, P.J. Picone, T.R. Thurston, G. Shirane, Y. Endoh, M. Sato, K. Yamada, Y. Hidaka, M. Oda, Y. Enomoto, M. Suzuki, and T. Murakami, *Phys. Rev. B* **38**, 6614 (1988).
- ³³D.S. Dessau, T. Saitoh, P. Villeda, C.H. Park, Z.-X. Shen, Y. Moritomo, and Y. Tokura, *J. Phys. Chem. Solids* **59**, 1917 (1998).
- ³⁴H.S. Choi, Y.S. Lee, T.W. Noh, E.J. Choi, Y. Bang, and Y.J. Kim, *Phys. Rev. B* **60**, 4646 (1999); H.S. Choi, E.J. Choi, and Y.J. Kim, *Physica C* **304**, 66 (1998).
- ³⁵M. Grüninger, D. van der Marel, A. Damascelli, A. Erb, T. Nunner, and T. Kopp, *Phys. Rev. B* **62**, 12 422 (2000).
- ³⁶A. Damascelli, K. Schulte, D. van der Marel, and A.A. Menovsky, *Phys. Rev. B* **55**, R4863 (1997).
- ³⁷J. Lorenzana, J. Eroles, and S. Sorella, *Phys. Rev. Lett.* **83**, 5122 (1999).
- ³⁸A. Lanzara, P.V. Bogdanov, X.J. Zhou, S.A. Kellar, D.L. Feng, E.D. Lu, T. Yoshida, H. Eisaki, A. Fujimori, K. Kishio, J.-I. Shimoyama, T. Nodak, S. Uchida, Z. Hussain, and Z.-X. Shen, *Nature (London)* **412**, 510 (2001).
- ³⁹C.J. Stevens, D. Smith, C. Chen, J.F. Ryan, B. Podobnik, D. Mihailovic, G.A. Wagner, and J.E. Evetts, *Phys. Rev. Lett.* **78**, 2212 (1997).
- ⁴⁰Y. Zhang, N.P. Ong, P.W. Anderson, D.A. Bonn, R. Liang, and W. N. Hardy, *Phys. Rev. Lett.* **86**, 890 (2001).
- ⁴¹S. Uchida, T. Ido, H. Takagi, T. Arima, Y. Tokura, and S. Tajima, *Phys. Rev. B* **43**, 7942 (1991).
- ⁴²G.A. Sawatzky, *Nature (London)* **342**, 480 (1989).